Supplement of Atmos. Chem. Phys., 18, 11345–11361, 2018
https://doi.org/10.5194/acp-18-11345-2018-supplement

Atmospheric Chemistry and Physics
Open Access
EGU

Supplement of

Size-resolved mixing state of black carbon in the Canadian high Arctic and implications for simulated direct radiative effect

John K. Kodros et al.

Correspondence to: John K. Kodros (jkodros@atmos.colostate.edu)

Supplement of "**Size-resolved mixing state of black carbon in the Canadian high Arctic and implications for simulated direct radiative effect**"

Details of observational flights

Table S1 provides additional details of the subset of flights used in this study. The six flights detailed in Table S1 correspond to the flight tracks in the map in Figure 1 of the main text.

Determination of the fraction of total aerosols containing rBC vs aerosol diameter (expanded discussion).

The following are the steps (with a graphical example in Figure S1) of how the fraction of total aerosols containing rBC vs aerosol diameter was determined.

1. The number size distribution of rBC cores was determined from SP2#1. An example is shown in Figure S1, panel (A).
2. The coating thickness as a function rBC core diameter was determined from SP2#2. An example is shown in Figure S1, panel (B). As discussed in the manuscript and in the Supplemental Information, there is some uncertainty in determining the coating thickness for small particles. To measure the impact of this uncertainty a sensitivity test was done with maximum and minimum coating cases. These are shown in grey while the median case is shown in green. In addition, for larger particles outside the detection range of SP2#2 (rBC core diameter > 220nm), the median coating for the largest detectable particle (rBC core diameter = 220nm) was used.
3. The results from Steps 1 and 2 were combined to give the number size distribution of rBC containing particles. This was done by fitting the coating size distribution (panel B) to get an equation giving coating as a function of core diameter. This function was then used to calculate a total size for each particle. Shown in Figure S1, panel (C), is the number size distribution of rBC containing particles based on this process and the data in panels (A) and (B). Note that the x-axis represents the total diameter (i.e. the radius of the rBC core plus twice the thickness of the coating).
4. The fraction of total aerosols containing rBC vs aerosol diameter was determined by dividing the number size distribution of rBC containing particles from Step 3 by the number size distribution of the total aerosol determined with the UHSAS. Shown in Figure S1, panel (D) is an example of a number size distribution of the total aerosol determined with the UHSAS, and shown in panel (E) is the fraction of total aerosols containing rBC vs aerosol diameter determined with the data shown in panels (C) and (D).

Bounding cases of coating thickness for rBC cores less than 140 nm and resulting direct radiative effect

To determine the coating thickness as a function of rBC core diameter (as shown in Figure 2) the rBC cores were binned in 5 nm intervals and the median coating thickness across all flights and measurements was calculated for each bin. However, since there is a known bias toward thicker coatings at smaller rBC cores sizes, this median value is not accurate for rBC core diameters less than 140 nm. This is due in large part to the fact that small particles with thin or no coatings do not produce a detectable elastic scattering signal and therefore cannot have a coating thickness determined for them. To overcome this, conservative minimum and maximum coating thickness were also calculated for each bin. We estimated minimum coating thicknesses by assuming that all particles for which a coating thickness could not be determined were bare rBC particles. We estimated maximum coating thicknesses by assuming that all particles for which a coating thickness could not be determined had the median coating thickness from the successful fits. For bins where >90% of all particles could be successfully assigned a coating thickness, the minimum, maximum, and median were very similar. For smaller particles, where <90% could be assigned a coating thickness, the differences were significant. In order to overcome the known biases in the median for these cases, we used the minimum and maximum coating values as bounding values. The median coating value for bins with <90% successful fits was set as the overall median coating thickness from bins where the LEO success rate was 90% or greater. For rBC core diameters larger than 220 nm, the median value for a 220 nm particle was used. The results from this are shown in Figure S1. This process was carried out separately for each flight and the average of all flights (black line in Figure S1) was used for the GEOS-Chem simulations.

Table S1 presents the resulting direct radiative effect (DRE) for the r_{shell}-*constrained* and *fBC-constrained* mixing states considering the minimum, median, and maximum coating assumptions. Overall there is not a large difference in DRE across the minimum and maximum assumptions. This is due to most of the optical extinction taking place at particle diameters greater than 140 nm.

April mean albedo

Figure S2 shows April climatological mean albedo in the Arctic. Albedo climatology is derived from MODIS retrievals from years 2002-2007 and described in Heald et al. (2014). Ocean albedo is held constant at a value of 0.07; however, sea ice alters the spatial distribution of albedo. Estimates of DRE are likely sensitive to albedo climatology.

Variability of coating thickness with altitude for all flights

Figure S3 shows coating thickness as a function of altitude for each of the 6 flights considered here.

Table 1 Time, location, and duration of the portion of POLAR6 flights used in this study and shown in Figure 1

Period	Flight	Date	Takeoff/Landing location	Takeoff (UTC)	Landing (UTC)	Flight Time
Spring, 2015	2	7.4.2015	Alert (82.5° N, 62.3° W)	16:31:57	20:48:12	4:16:15
	3	8.4.2015	Alert (82.5° N, 62.3° W)	13:51:19	16:43:44	2:52:25
	4	8.4.2015	Alert (82.5° N, 62.3° W)	17:53:04	21:22:43	3:29:39
	5	9.4.2015	Alert (82.5° N, 62.3° W)	13:50:12	17:47:34	3:57:22
	6	11.4.2015	Eureka (80.0° N, 85.9° W)	15:57:28	21:16:05	5:18:37
	7	13.4.2015	Eureka (80.0° N, 85.9° W)	15:14:27	20:52:05	5:37:38

Table S2. The DRE for measurement-constrained mixing states using the minimum, median, and maximum assumptions.

Simulation		DRE [W m^{-2}]
fBC-constrained	min	-1.462
	med	-1.454
	max	-1.455
r_{shell}-constrained	min	-1.593
	med	-1.591
	max	-1.588

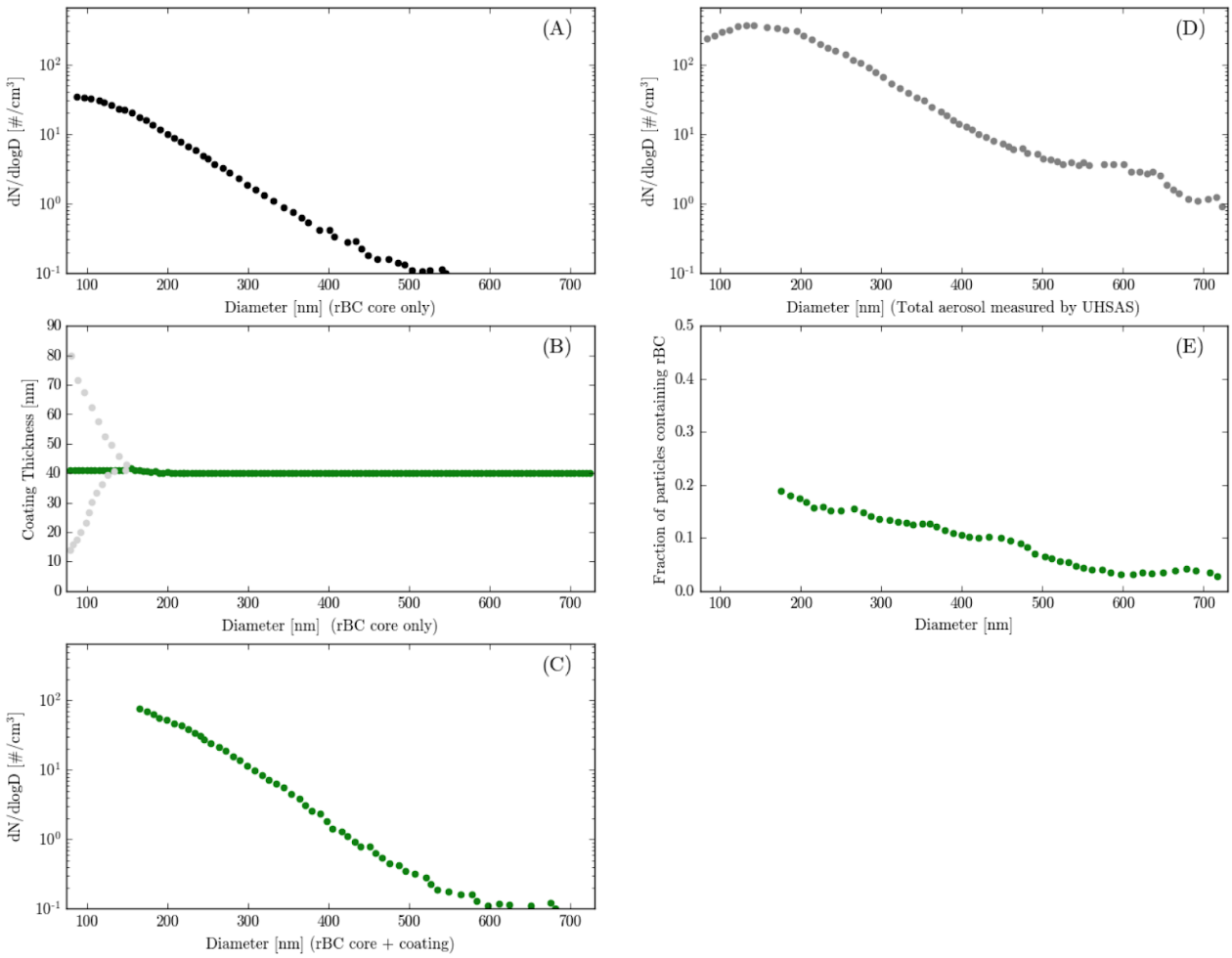

Figure S1. Steps in the determination of the size-dependent fraction of particles containing rBC. Panel **(A)** shows the measured number distribution of rBC cores from SP2#1. Panel **(B)** shows measured coating thickness as a function of core size from SP2#2. Note that the grey points show minimum and maximum bounding cases for small particle sizes. Panel **(C)** shows the number distribution for rBC-containing particles with the x-axis being total particle size (core diameter plus twice the coating thickness). Panel **(D)** is the total aerosol number distribution measured by the UHSAS. Panel **(E)** is the fraction of particles containing rBC calculated from the data in panels **(C)** and **(D)**. Data used is from flight 5.

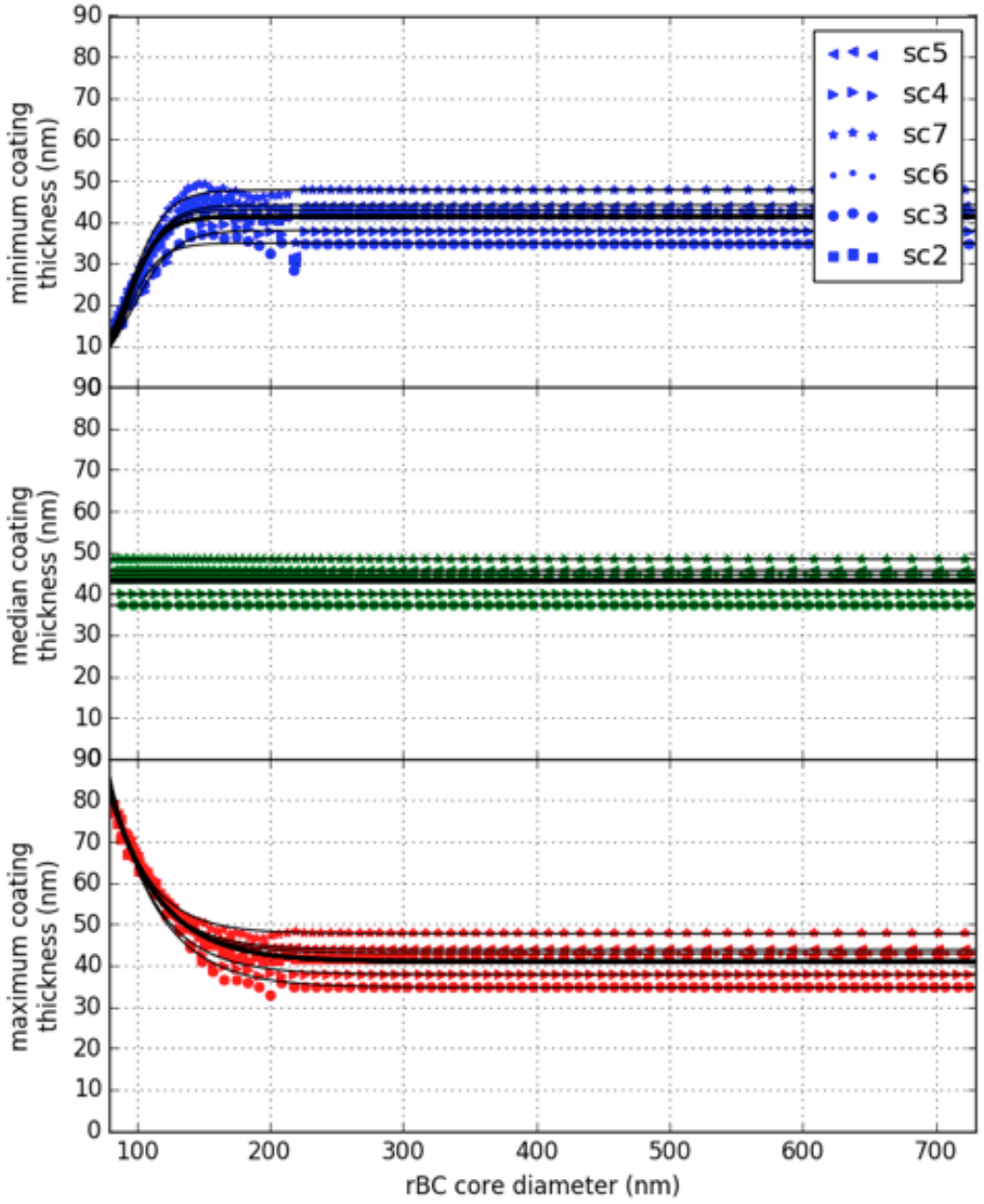

Figure S2. Minimum, median, and maximum possible coating thicknesses as a function of rBC core diameter. In each scenario, there are separate symbols and a fit line for each flight, and there is a heavy black line which is the fit to all flights combined.

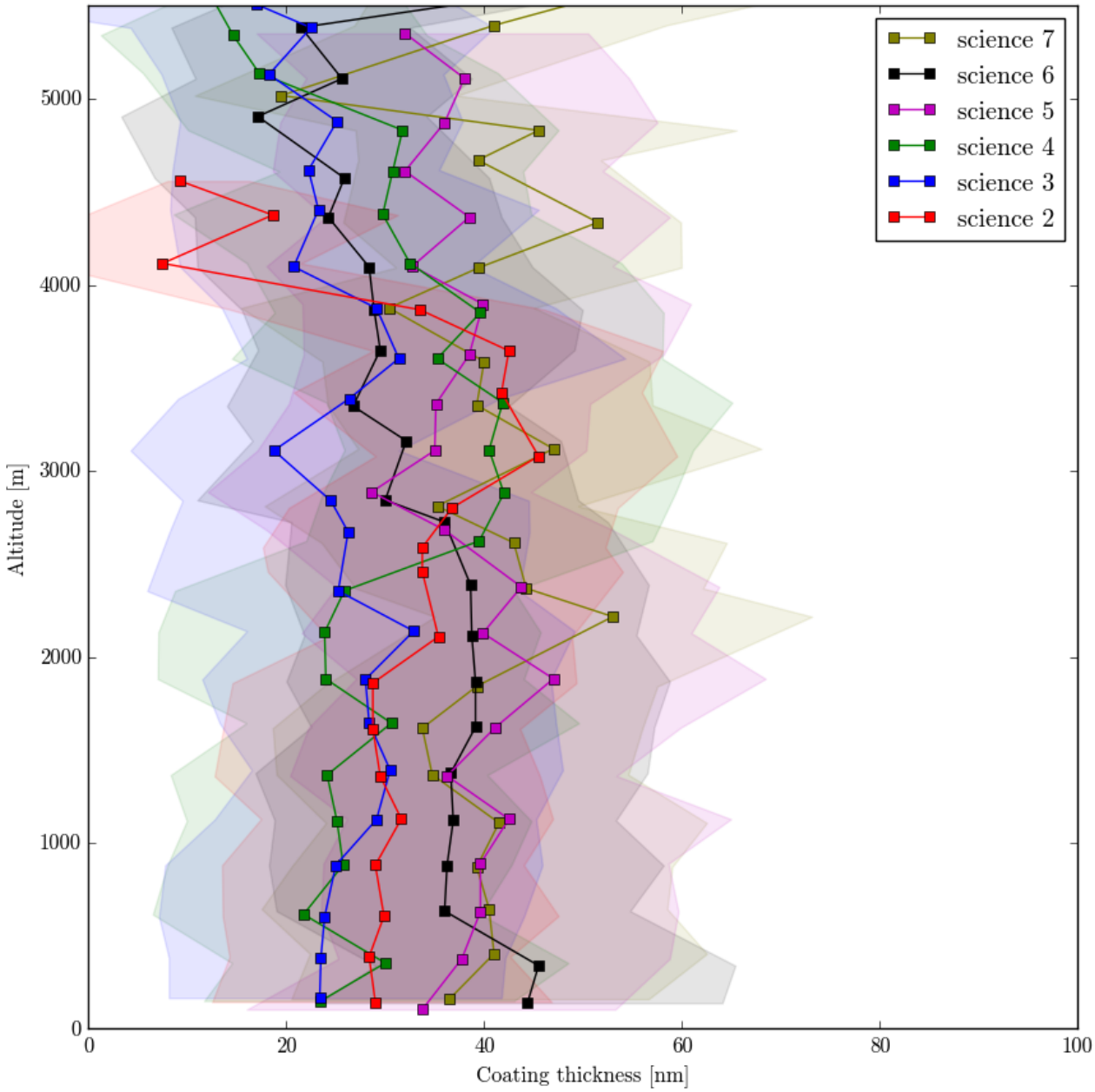

Figure S3. Coating thickness as a function of altitude for rBC cores from 170-190nm. This range of core sizes was chosen because in this range the LEO fitting is successful for >95% of detected particles, and significant number of particles are detected. The solid lines are median coating thicknesses while the shaded areas show the 25th-75th percentile range.

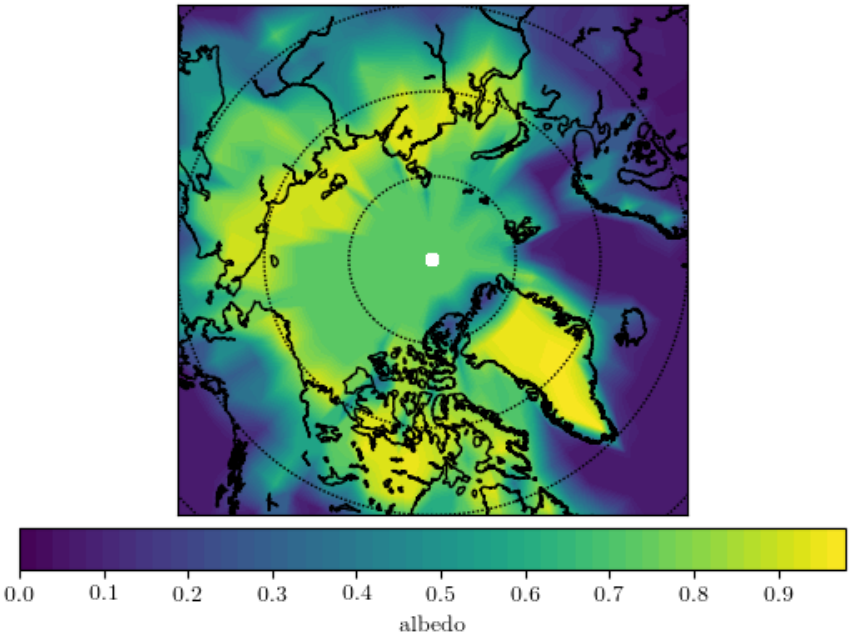

Figure S3. April mean albedo for visible wavelengths